MOLECULAR IMAGING AND BIOLOGY

Mol Imaging Biol (2019) 21:835–841
DOI: 10.1007/s11307-018-01312-3

Published Online: 8 January 2019

RESEARCH ARTICLE

Optical Imaging of Triple-Negative Breast Cancer Cells in Xenograft Athymic Mice Using an ICAM-1-Targeting Small-Molecule Probe

Yanqiu Zhang,[1,2] Mengru Wang,[1] Wanhua Liu,[1] Xin Peng[1]

[1]*Jiangsu Key Laboratory of Molecular and Functional Imaging, Department of Radiology, Zhongda Hospital, School of Medicine, Southeast University, Nanjing, 210009, Jiangsu, People's Republic of China*
[2]*Department of Radiology, Nanjing Drum Tower Hospital, The Affiliated Hospital of Nanjing University Medical School, Nanjing, 210002, Jiangsu, People's Republic of China*

Abstract

Purpose: The development of early, accurate diagnostic strategies for triple-negative breast cancer (TNBC) remains a significant challenge. Intercellular adhesion molecule-1 (ICAM-1) overexpressed in human TNBC cells is a potential molecular target and biomarker for diagnosis. In this study, small-molecule probe (denoted as γ3-Cy5.5) constructed with a short 17-mer linear peptide (γ3) and near-infrared fluorescence (NIRF) dye cyanine 5.5 (Cy5.5) was used to detect the expression of ICAM-1 *in vitro* and *in vivo*, and to diagnose TNBC *via* NIRF imaging.

Procedures: Western blotting and flow cytometric analysis were used for the detection of ICAM-1 expression in MDA-MB-231 and MCF-7 cells. The cytotoxicity of the small-molecule probe γ3-Cy5.5 was detected using the CCK8 assay. The *in vitro* targeting of the small-molecule probe γ3-Cy5.5 was verified *via* flow cytometry and a laser scanning confocal microscope. Finally, the targeting of small-molecule probe *in vivo* and *ex vivo* was observed by NIRF imaging.

Results: Western blotting and flow cytometry demonstrate that ICAM-1 was highly expressed in the MDA-MB-231 TNBC cell line. Laser confocal microscopy and flow cytometry results show that TNBC cells have an increased cellular uptake of γ3-Cy5.5 compared to the control probe γ3S-Cy5.5. With *in vivo* NIRF, a significantly higher Cy5.5 signal appeared in the tumors of mice administered γ3-Cy5.5 than those treated with γ3S-Cy5.5. The target-to-background ratio observed on the NIRF images was significantly higher in the γ3-Cy5.5 group (10.2, 13.6) compared with the γ3S-Cy5.5 group (4.4, 4.0) at 1 and 2 h, respectively.

Conclusions: This is the first report of the use of ICAM-1-specific small-molecule probe for *in vivo* NIRF optical imaging of TNBC. This method provides a noninvasive and specific strategy for the early diagnosis of TNBC.

Key words: Triple-negative breast cancer, ICAM-1, Near-infrared fluorescence imaging, Small-molecule probe

Introduction

Breast cancer is the most frequently diagnosed cancer among women worldwide and is also the leading cause of cancer deaths [1]. Triple-negative breast cancer (TNBC) is a type of breast cancer with low or no expression of the estrogen receptor,

Yanqiu Zhang and Mengru Wang contributed equally to this work.

Correspondence to: Wanhua Liu; *e-mail:* liuwanhua.com@126.com

progesterone receptor, and epidermal growth factor receptor-2. The clinical features and tumor biology are different from other types of breast cancer. TNBC accounts for approximately 1–20 % of all breast cancers [2–4]. The risk of recurrence of TNBC after 5 years is significantly higher than that of other types of breast cancer [5]. The high mortality rate of TNBC is attributed to its aggressive proliferation and metastasis, and lack of effective treatment options [6–8]. Therefore, early diagnosis and treatment play an important role in the prognosis of TNBC, and it is urgent to identify a simple and accurate imaging method for the early diagnosis of TNBC.

Molecular imaging technology is a new research field encompassing the development and fusion of medical imaging technology and molecular biology methods such as material science, chemistry, and bioengineering. This method plays an important role in the diagnosis, treatment evaluation, and monitoring of functional molecule activity of TNBC *in vivo*. Optical molecular imaging has many advantages, such as high sensitivity, real-time visualization, fast imaging, simple operation, low cost, and lack of radioactive hazards, and it can simultaneously observe multi-molecular events. This method is important for observing the occurrence, development, and metastasis of tumors *in vivo*, in addition to monitoring the expression of specific molecules and genes [9, 10]. Therefore, there is a need to develop a reagent that targets TNBC and can be monitored by optical imaging.

Intercellular adhesion molecule-1 (ICAM-1) is a cell surface transmembrane glycoprotein receptor belonging to the immunoglobulin superfamily. ICAM-1 plays a role in the process of cancer metastases and affects tumor prognosis and progression in various types of cancer [11–14]. In recent years, studies have demonstrated higher expression levels of ICAM-1 in TNBC cell lines and patients compared to those with other subtypes of breast cancer [15–17]. Guo and coworkers reported higher expression levels of ICAM-1 in TNBC cell line (MDA-MB-231) than in non-TNBC cell line (MCF-7) and demonstrated that ICAM-1 molecule can be a new target for TNBC diagnosis and treatment [6]. Garnacho et al. synthesized a short, 17-mer linear peptide containing the ICAM-1-binding sequence of the fibrinogen gamma chain (NNQKIVNLKEKVAQLEA, called γ3) which binds effectively and specifically to ICAM-1 in humans and mice [18].

The aim of this study was to detect the expression of ICAM-1 *in vivo* and *in vitro* using the combination of fluorescent dye Cy5.5 and γ3 (γ3-cy5.5), and to diagnose TNBC *via* near-infrared fluorescence (NIRF) imaging. This is the first time that an ICAM-1-specific small-molecule probe has been used for the *in vivo* NIRF optical imaging of TNBC. This method provides a noninvasive and specific method for the early diagnosis of TNBC.

Materials and Methods

Cell Culture

The human TNBC cell line (MDA-MB-231) and human non-TNBC cell lines (MCF-7) were obtained from the American Type Culture Collection (ATCC, Manassas, VA). All cells were cultured in high-glucose Dulbecco's Modified Eagle Medium (DMEM) (GIBCO, Grand Island, NY) supplemented with 10 % fetal bovine serum (FBS, GIBCO) and 1 % Pen/Strep (10,000 U penicillin, 10 mg/ml streptomycin) at 37 °C in an atmosphere containing 5 % (*v*/*v*) CO_2.

ICAM-1 Expression

For the western blotting analysis, cells were lysed in radioimmunoprecipitation assay (aka RIPA) buffer and equal amounts of protein (20 μg) were loaded per well. Electrophoresis was performed using an 8 % polyacrylamide separating gel with a 4 % stacking gel, and proteins were transferred to polyvinylidene difluoride membranes (Immobilon P, Millipore, Eschborn, Germany) by tank blotting. After 2 h incubation at room temperature in blocking solution, membranes were incubated overnight at 4 °C with the primary antibody G5 (sc-8439; Santa Cruz, Heidelberg, Germany), diluted 1:300. The secondary horseradish peroxidase-conjugated anti-mouse-IgG was obtained from GE Healthcare (Port Washington, NY; 1:5000). Densitometric analysis was performed using ImageJ software (National Institutes of Health, Bethesda, MD).

Flow cytometric analysis was used for the detection of ICAM-1 expression in MDA-MB-231 and MCF-7 cells. The cells, at a concentration of 1×10^5 cells per 100 ml of PBS plus 1 % FCS were incubated with phycoerythrin/anti–ICAM-1 antibody (Biolgend Catalog) for 1 h at room temperature. Then, cells were washed three times in PBS containing 1 % FCS, resuspended in 1 % paraformaldehyde and evaluated using a BD FACSCalibur flow cytometer (BD Biosciences).

Synthesis of the Small-Molecule Probes γ3-Cy5.5 and γ3S-Cy5.5

γ3 is a 17-mer peptide containing the ICAM-1-binding sequence of fibrinogen [NNQKIVNLKEKVAQLEA] and γ3s is a control peptide containing the γ3 sequence in scrambled order [ALENAEVQNLVKKI] [19]. The probes were synthesized and labeled with the fluorescent dye Cy5.5 at the C-terminus. All peptides (γ3-Cy5.5 and γ3S-Cy5.5) had a minimum purity of 95 % and were synthesized and fluorescently labeled by Shanghai Sangon Biological Engineering Technology & Services Co. Ltd. (Shanghai, China).

Cytotoxicity of the γ3-Cy5.5 and γ3S-Cy5.5

The cytotoxicity of the small-molecule probe γ3-Cy5.5 was detected using the CCK8 assay. In brief, the MDA-MB-231 cells were seeded in 96-well plates (Corning Incorporated, USA) at a density of 1×10^5 cells per well in 200 μl of

culture medium and were maintained for 24 h. Six duplicate wells were set for each concentration. The cells were then incubated in medium containing the small-molecule probe for 1 day. Then, 10 μl of CCK8 solution (Sigma-Aldrich, USA) was added to each well and the plates were incubated for 2 h. The optical density at a wavelength of 470 nm (OD470 nm) was detected using a microplate spectrophotometer (Thermo Fisher Scientific, USA).

ICAM-1 Immunofluorescence Staining

MDA-MB-231 cells (5×10^4) were plated in 24-well plates with 1 ml medium overnight at 37 °C. After medium was removed, cells were incubated with γ3-Cy5.5 and γ3S-Cy5.5 at 2.5, 5, 10, or 20 μM for 30 min at 37 °C. Afterwards, cells were rinsed with PBS three times and fixed with 4 % formaldehyde in PBS at room temperature for 15 min. DAPI was used to stain the cell nuclei. Finally, immunofluorescent stained samples were dried overnight in the dark and photographed using a laser scanning confocal microscope.

Detection of the Small-Molecule Probe via Flow Cytometry

MDA-MB-231 cells (1×10^5 cells per 100 μl of PBS plus 1 % FCS) were incubated with γ3-Cy5.5 and γ3S-Cy5.5 at 2.5, 3, 4, 5, 10, or 20 μM for 30 min at 37 °C. Then, cells were washed three times in PBS containing 1 % FCS, resuspended in 1 % paraformaldehyde and evaluated using a BD FACSCalibur flow cytometer (BD Biosciences). Flow cytometry was performed to test the binding of the γ3-Cy5.5 to MDA-MB-231 cells *versus* MCF-7 cells. MCF-7 cells were incubated with γ3-Cy5.5 at 5 μM for 30 min at 37 °C. The results were determined *via* flow cytometer. To further evaluate the binding properties of the small-molecule probe, competitive inhibition experiments were carried out. MDA-MB-231 cells (10^5 cells per 100 μl of PBS plus 1 % FCS) were incubated with γ3 (50 μM) containing unlabeled fluorescent dyes and γ3-Cy5.5 (10 μM) for 30 min at 37 °C. The bound small-molecule probe was detected as described above.

MDA-MB-231 Tumor Xenograft Model

All animal experiments were carried out in accordance with the protocols evaluated and approved by the Institutional Animal Care and Use Committee (IACUC) of the Medical School of Southeast University. Four to five-week-old female BALB/c nu/nu mice were obtained from the Yangzhou Laboratory Animal Center (Yangzhou, China). The TNBC model was established by subcutaneous injection (sc) of 5×10^6 MDA-MB-231 cells into the fourth mammary fat pad of athymic nude mice.

In Vivo and Ex Vivo NIRF Imaging

In vivo optical imaging was performed on two groups of tumor-bearing mice intravenously injected with γ3-cy5.5 and γ3S-cy5.5 (200 μl/mouse). NIRF images were captured using a Maestro *in vivo* imaging system (CRi, Woburn, MA, USA; Orange: excitation, 605 nm, emission, 640–820 in 10 nm steps) and analyzed using Maestro 2.10.0 Software (CRi, Woburn, MA, USA). NIRF signal intensity was quantified as counts per second per pixel. After 2 h of circulation, the mice were euthanized and surgically dissected. The tumors and organs were used for *ex vivo* fluorescence imaging. All near-infrared fluorescence images were acquired using 1000-ms exposure time. For the analysis of signal changes at a series of time points and in different groups, oval regions of interest (ROIs) were manually drawn on the *in vivo* and *ex vivo* images in the tumor or organ site, and the ear site. The target-to-background ratio (TBR) was calculated as follows: (ROI value from the tumor or organ site)/(ROI value from the ear site).

Statistical Analysis

Quantitative data are presented as means ± SD. Differences were compared using an unpaired *t* test. A P value ≤ 0.05 was considered statistically significant.

Results

Western blot analysis of ICAM-1 expression in the human TNBC cell line (MDA-MB-231) and human non-TNBC cell line (MCF-7) show broad bands ranging from approximately 80 to 120 kD. This is due to different levels of glycosylation, which has been described by various authors [20, 21]. ICAM-1 expression was nearly threefold higher in MDA-MB-231 cells (quantified by Western blot analysis; $P < 0.05$) than that in MCF-7 cells (Fig. 1a and b). Flow cytometric analysis further confirmed a much higher expression of ICAM-1 in MDA-MB-231 cells than in MCF-7 cells (Fig. 1c). Values from three independent experiments showed an average ICAM-1 surface protein of 99.1 ± 1.0 % in MDA-MB-231 cells and 65.1 ± 2.4 % in MCF-7 cells (Fig. 1d), which was a statistically significant difference ($P < 0.01$).

The cytotoxicity of γ3-Cy5.5 and γ3S-Cy5.5 was evaluated by incubating the small-molecule probes with TNBC cells (MDA-MB-231) for 24 h. The results showed that MDA-MB-231 cell viability remained above 92 % when the concentration of γ3-Cy5.5 and γ3S-Cy5.5 reached 100 μM (Fig. 2a), indicating excellent biocompatibility. Immunofluorescence staining was performed to test the binding properties of γ3-Cy5.5. MDA-MB-231 cells were incubated with various concentrations of γ3-Cy5.5 and γ3S-Cy5.5 and most of the MDA-MB-231 cells bound the γ3-Cy5.5 probe. However, a low signal was observed for γ3S-Cy5.5, and the

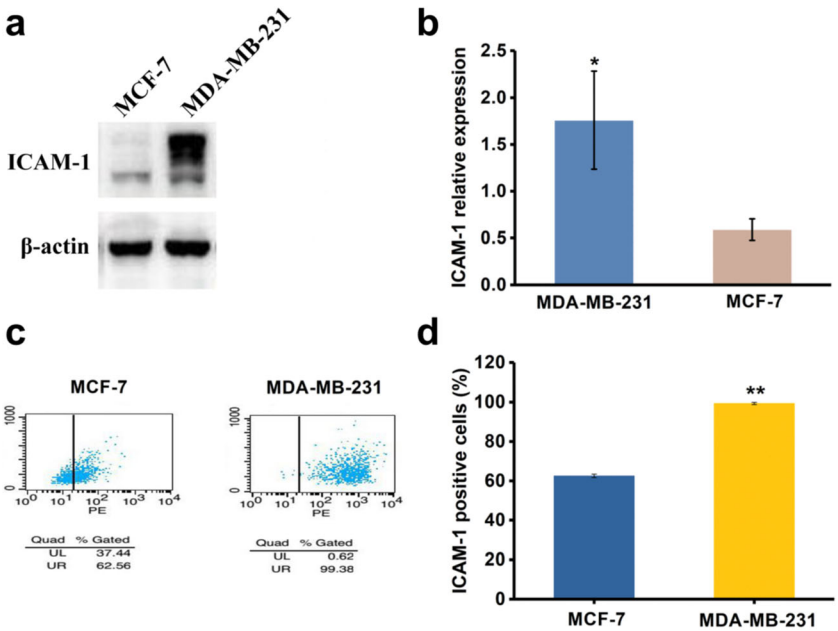

Fig. 1. **a** Western blot analysis of ICAM-1 expression in the human TNBC cell line (MDA-MB-231) and human non-TNBC cell line (MCF-7). Tubulin expression was used as a loading control. **b** Quantification of ICAM-1 protein expression by the densitometric analysis (*$P < 0.05$). **c** Flow cytometric analysis of ICAM-1 expression. **d** Quantification of ICAM-1 protein expression by flow cytometry (**$P < 0.01$).

fluorescent signal increased with increasing amounts of γ3-Cy5.5 (2.5–20 μM; Fig. 2b). Flow cytometric analysis further confirmed the binding properties of γ3-Cy5.5. Values from three independent experiments showed a statistically significant difference in the average binding properties of the various concentrations of γ3-Cy5.5 and γ3S-Cy5.5 in MDA-MB-231 cells (**$P < 0.01$; Fig. 2c). In addition, γ3-Cy5.5 exhibited weak binding to MCF-7 cells (Fig. 2d), due to the low expression of ICAM-1 on MCF-7 cells.

To further assess the binding properties of γ3-Cy5.5, competitive binding between γ3-Cy5.5 and the unlabeled γ3 peptide was examined. After incubation with the unlabeled γ3 peptide as a competitor, significantly less γ3-Cy5.5 fluorescence was detected in MDA-MB-231 cells (Fig. 2e), indicated that the combination of γ3-Cy5.5 and MDA-MB-231 cells is mainly due to that the γ3 peptide can specifically bind to MDA-MB-231 cells.

We ultimately examined the use of γ3-cy5.5 for the targeted imaging of TNBC tumors *in vivo via* NIRF imaging using a xenograft TNBC mouse model. NIRF imaging was performed on two groups of mice treated with either γ3-Cy5.5 or γ3S-Cy5.5. Each group was scanned at 0, 1, and 2 h after injection of the imaging probes, respectively. Compared with the pre-injection imaging at baseline, a significantly higher Cy5.5 signal appeared in the tumors of mice administered γ3-Cy5.5 where those treated with γ3S-Cy5.5 exhibited no significant Cy5.5 signal aggregation in the tumor site at 1 or 2 h post-injection (Fig. 3a). The TBR observed on the NIRF images was significantly higher in the γ3-Cy5.5 group compared with the γ3S-Cy5.5 group at different time points (Fig. 3b). Furthermore, *ex vivo* images showed higher tumor accumulation of γ3-Cy5.5 than γ3S-Cy5.5 (Fig. 3c). The TBR in different organs illustrated that there was no significant difference between the γ3-Cy5.5 group and the γ3S-Cy5.5 group except at the tumor sites (Fig. 3d). Although the probe had a certain distribution in the liver and kidneys, this is an inevitable and expected occurrence, and is seen with other small-molecule probes. This is likely due to the fact that the liver and kidneys are metabolically active organs and almost all peptides are soluble in nature [22, 23]. Furthermore, asymmetric cyanine dyes accumulate in and are cleared from the liver and kidneys [24].

Discussion

In recent years, studies have demonstrated higher levels of ICAM-1 expression in TNBC cell lines and patients than in those with other subtypes of breast cancer [6]. Many studies have shown that ICAM-1 plays a role in the process of tumor metastasis. What's more, overexpression of ICAM-1 can enhance tumor growth and have a stimulatory effect on their progression [25–27]. In this study, we proved that ICAM-1 exhibited higher expression in TNBC cell lines (MDA-MB-231) than in non-TNBC cell lines (MCF-7) *via* western blotting and flow cytometry. In addition, we imaged TNBC tumors from MDA-MB-231 xenograft nude mice successfully with the small-molecule probe γ3-Cy5.5.

With the rapid development of molecular imaging, small molecular probes have become a research hotspot. The small probes are small proteins that have been engineered to bind to targeted proteins or short peptides. These molecules have been developed into novel targeted drugs for the treatment of a variety of diseases [28]. Compared with antibodies, small molecules

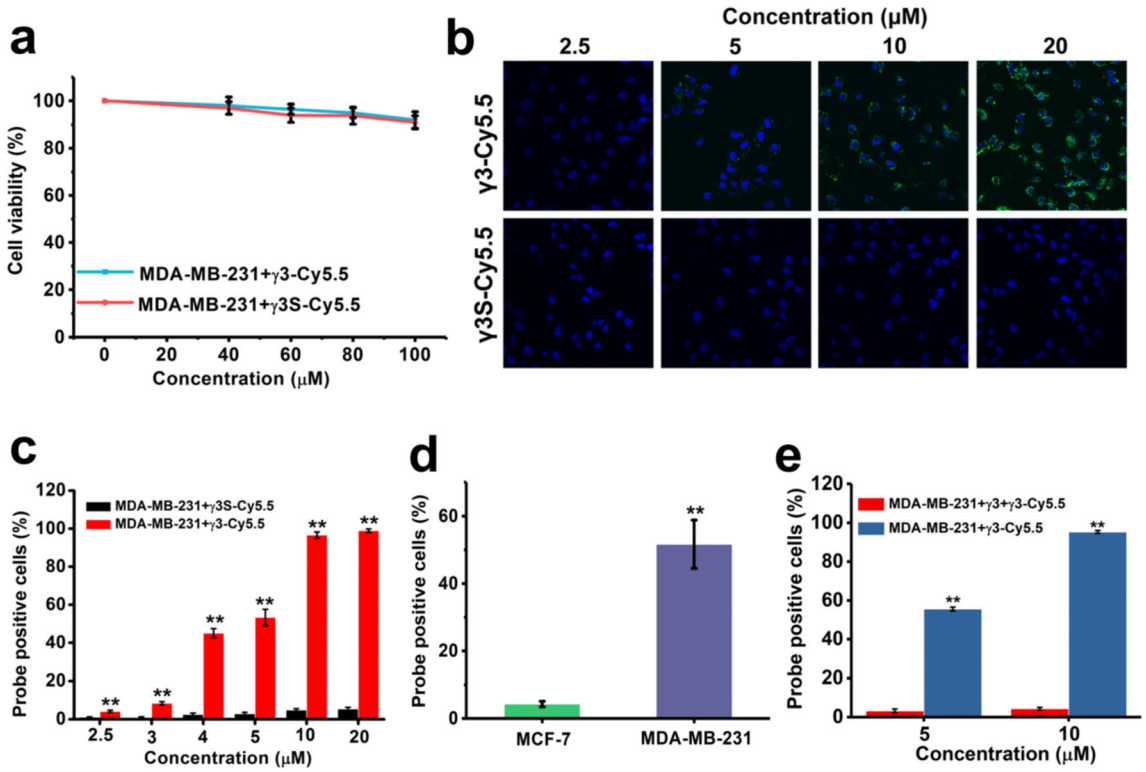

Fig. 2. **a** Viability of MDA-MB-231 cells incubated with γ3-Cy5.5 and γ3S-Cy5.5 at different concentrations after 24 h. **b** Confocal laser scanning microscopy of MDA-MB-231 cells incubated with various concentrations (2.5, 5, 10, and 20 μM) of γ3-Cy5.5 and γ3S-Cy5.5 for 30 min. Blue and green fluorescence are from DAPI and Cy5.5, respectively. **c** Quantification of the average binding properties of the various concentrations (2.5, 3, 4, 5, 10, and 20 μM) of γ3-Cy5.5 and γ3S-Cy5.5 in MDA-MB-231 cells by flow cytometry. **d** Quantification of the average binding properties of 5 μM γ3-Cy5.5 in MDA-MB-231 cells and MCF-7 cells by flow cytometry. **e** Competitive binding imagine between γ3-Cy5.5 and the unlabeled γ3 peptide (**$P < 0.01$).

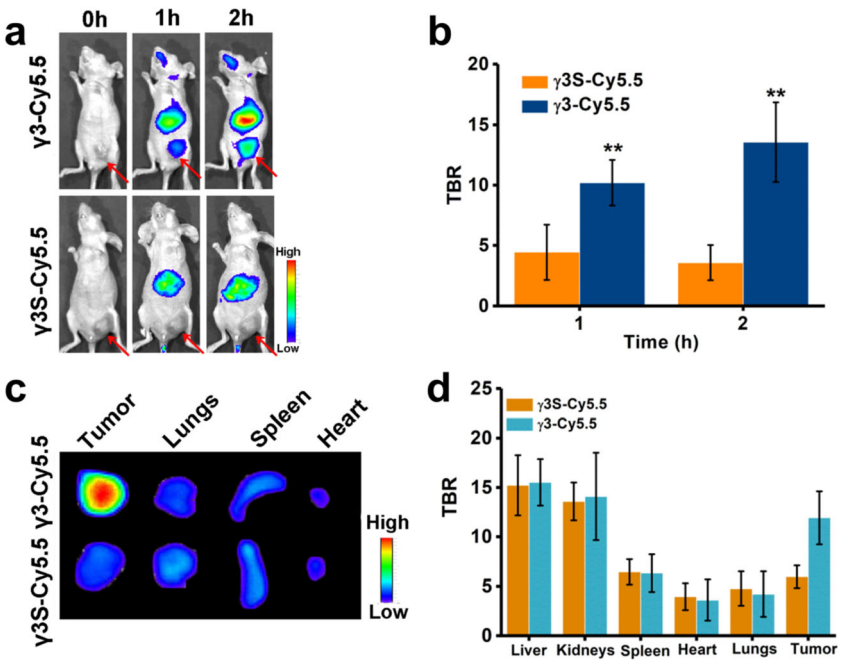

Fig. 3. **a***In vivo* NIRF of mice with subcutaneous MDA-MB-231 xenografts receiving γ3-Cy5.5 and γ3S-Cy5.5. Mice were imaged at 0, 1, and 2 h after injection. **b** The TBR observed on the *in vivo* NIRF images. **c***Ex vivo* NIRF imaging and **d** TBR in the tumors, lungs, spleens, and hearts after i.v. administration of γ3-Cy5.5 and γ3S-Cy5.5 into MDA-MB-231-bearing mice for 2 h. ($n = 3$; **$P < 0.01$).

have advantages as targeted drug delivery vehicles because of their small size, efficient tissue penetration, and low immunogenicity [29]. In this study, the small-molecule probe (denoted as γ3-cy5.5) constructed by a short 17-mer linear peptide (γ3) and near-infrared fluorescence dye cyanine 5.5 (Cy5.5) was used to diagnose TNBC *via* NIRF imaging. *In vitro* and *in vivo* experiments showed that γ3-Cy5.5 effectively accumulated in TNBC cells and, therefore, may be a good candidate for the noninvasive imaging of TNBC using NIRF imaging. In addition, molecular imaging technology is a new research field formed with the development and fusion of medical imaging technology and molecular biology, material science, chemistry, and bioengineering, *etc.*, which plays an important role in the diagnosis, treatment evaluation and monitoring of functional molecules *in vivo* activity rules of TNBC. Among them, optical molecular imaging has the advantages of high sensitivity, real-time visualization, rapid imaging, simple operation, low cost, no radiation damage, and simultaneous observation of multi-molecular events, and has gradually become an ideal method to study the changes of molecular level in tumor cells and live animal imaging [30].

The application of molecular diagnostic techniques to the study of tumor development and biological behavior at the molecular level has become a current research focus [31]. Molecular imaging methods using targeted probes can be used to diagnose the disease at the molecular level in a noninvasive manner and provide early diagnostic data on the disease. This is the first report on the use of an ICAM-1-specific small-molecule probe for *in vivo* NIRF optical imaging of TNBC. This method provides a noninvasive and specific strategy for the early diagnosis of TNBC.

Conclusions

We report a near-infrared fluorescence dye cyanine 5.5 (Cy5.5) labeled small-molecule probe (denoted as γ3-Cy5.5) and its use for the NIRF imaging of ICAM-1 expression in TNBC xenograft nude mice. *In vitro* experiments show that γ3-Cy5.5 exhibited suitable biocompatibility and effectively accumulated in TNBC cells. With *in vivo* NIRF, a significantly higher Cy5.5 signal appeared in the tumors of mice administered γ3-Cy5.5 than those treated with γ3S-Cy5.5. The TBR observed on the NIRF images was significantly higher in the γ3-Cy5.5 group (10.2, 13.6) compared with the γ3S-Cy5.5 group (4.4, 4.0) at 1 and 2 h, respectively. This study provides a noninvasive and specific method for the early diagnosis of TNBC. In the future, ICAM-1 molecular targets will provide new ideas for the treatment of TNBC.

Funding Information. This study received financial support from the National Key Basic Research Program of China (973 Program), China (2014CB744504).

Compliance with Ethical Standards

Conflict of Interest

The authors declare that they have no conflict of interest.

References

1. Bray F, Ferlay J, Soerjomataram I et al (2018) Global Cancer Statistics 2018: GLOBOCAN estimates of incidence and mortality worldwide for 36 cancers in 185 countries. Ca-Cancer J Clin. https://doi.org/10.3322/caac.21492
2. Foulkes WD, Smith IE, Reisfilho JS (2010) Triple-negative breast cancer. Wien Med Wochenschr 160:174–181
3. Carey L, Winer E, Viale G, Cameron D, Gianni L (2010) Triple-negative breast cancer: disease entity or title of convenience? Nat Rev Clin Oncol 7:683–692
4. Morris GJ, Naidu S, Topham AK et al (2010) Differences in breast carcinoma characteristics in newly diagnosed African-American and Caucasian patients: a single-institution compilation compared with the National Cancer Institute's Surveillance, Epidemiology, and End Results database. Cancer 110:876–884
5. Dent R, Trudeau M, Pritchard KI et al (2018) Triple-negative breast cancer: clinical features and patterns of recurrence. Clin Cancer Res 13:4429–4434
6. Guo P, Huang J, Wang L, Jia D, Yang J, Dillon DA, Zurakowski D, Mao H, Moses MA, Auguste DT (2014) ICAM-1 as a molecular target for triple negative breast cancer. Proc Natl Acad Sci U S A 111:14710–14715
7. Sørlie T (2004) Molecular portraits of breast cancer: tumour subtypes as distinct disease entities. Eur J Cancer 40:2667–2675
8. Shah SP, Roth A, Goya R, Oloumi A, Ha G, Zhao Y, Turashvili G, Ding J, Tse K, Haffari G, Bashashati A, Prentice LM, Khattra J, Burleigh A, Yap D, Bernard V, McPherson A, Shumansky K, Crisan A, Giuliany R, Heravi-Moussavi A, Rosner J, Lai D, Birol I, Varhol R, Tam A, Dhalla N, Zeng T, Ma K, Chan SK, Griffith M, Moradian A, Cheng SWG, Morin GB, Watson P, Gelmon K, Chia S, Chin SF, Curtis C, Rueda OM, Pharoah PD, Damaraju S, Mackey J, Hoon K, Harkins T, Tadigotla V, Sigaroudinia M, Gascard P, Tlsty T, Costello JF, Meyer IM, Eaves CJ, Wasserman WW, Jones S, Huntsman D, Hirst M, Caldas C, Marra MA, Aparicio S (2012) The clonal and mutational evolution spectrum of primary triple negative breast cancers. Nature 486:395–399
9. Hellebust A, Richardskortum R (2012) Advances in molecular imaging: targeted optical contrast agents for cancer diagnostics. Nanomedicine 7:429–445
10. Chen X (2011) Integrin targeted imaging and therapy. Theranostics 1:28–29
11. Cheng D, Liang B (2015) Intercellular adhesion molecule-1 (ICAM-1) polymorphisms and cancer risk: a meta-analysis. Iran J Public Health 44:615–624
12. Hua S (2013) Targeting sites of inflammation: intercellular adhesion molecule-1 as a target for novel inflammatory therapies. Front Pharmacol 4:127
13. Dymicka-Piekarska V, Kemona H (2009) Does colorectal cancer clinical advancement affect adhesion molecules (sP-selectin, sE-selectin and ICAM-1) concentration? Thromb Res 124:80–83
14. Hayes SH, Seigel GM (2009) Immunoreactivity of ICAM-1 in human tumors, metastases and normal tissues. Int J Clin Exp Pathol 2:553–560
15. Schröder C, Witzel I, Müller V, Krenkel S, Wirtz RM, Jänicke F, Schumacher U, Milde-Langosch K (2011) Prognostic value of intercellular adhesion molecule (ICAM)-1 expression in breast cancer. J Cancer Res Clin Oncol 137:1193–1201
16. Rosette C, Roth RB, Oeth P, Braun A, Kammerer S, Ekblom J, Denissenko MF (2005) Role of ICAM1 in invasion of human breast cancer cells. Carcinogenesis 26:943–950
17. Liu L, Sun M, Song D, Wang Z (2013) The genetic polymorphisms of intercellular cell adhesion molecules and breast cancer susceptibility: a meta-analysis. Mol Biol Rep 40:1855–1860
18. Garnacho C, Serrano D, Muro S (2012) A fibrinogen-derived peptide provides intercellular adhesion molecule-1-specific targeting and intraendothelial transport of polymer nanocarriers in human cell cultures and mice. J Pharmacol Exp Ther 340:638–647
19. Altieri DC, Duperray A, Plescia J, Thornton GB, Languino LR (1995) Structural recognition of a novel fibrinogen gamma chain sequence

(117-133) by intercellular adhesion molecule-1 mediates leukocyte-endothelium interaction. J Biol Chem 270:696–699
20. Chen C, Diao D, Liang G et al (2012) All-trans-retinoic acid modulates ICAM-1 N-glycan composition by influencing GnT-III levels and inhibits cell adhesion and trans-endothelial migration. PLoS One 7:e52975
21. Jiménez D, Rodanavarro P, Springer TA et al (2005) Contribution of N-linked glycans to the conformation and function of intercellular adhesion molecules (ICAMs). J Biol Chem 280:5854–5861
22. Maryelise C, Jingjing T, Yu JL et al (2013) Targeted delivery of proapoptotic peptides to tumor-associated macrophages improves survival. Pnas 110:15919–15924
23. Li J, Zhang Q, Pang Z, Wang Y, Liu Q, Guo L, Jiang X (2012) Identification of peptide sequences that target to the brain using in vivo phage display. Amino Acids 42:2373–2381
24. Hamann FM, Brehm R, Pauli J et al (2011) Controlled modulation of serum protein binding and biodistribution of asymmetric cyanine dyes by variation of the number of sulfonate groups. Mol Imaging 10:258–269
25. Zhang KE, Shujian GE, Lin X et al (2016) Intercellular adhesion molecule 1 is a sensitive and diagnostically useful immunohistochemical marker of papillary thyroid cancer (PTC) and of PTC-like nuclear alterations in Hashimoto's thyroiditis. Oncol Lett 11:1722–1730
26. Zhu XW, Gong JP (2013) Expression and role of icam-1 in the occurrence and development of hepatocellular carcinoma. Asian Pac J Cancer Prev 14:1579–1583
27. Kotteas EA, Boulas P, Gkiozos I, Tsagkouli S, Tsoukalas G, Syrigos KN (2014) The intercellular cell adhesion molecule-1 (icam-1) in lung cancer: implications for disease progression and prognosis. Anticancer Res 34:4665–4672
28. Löfblom J, Feldwisch J, Tolmachev V, Carlsson J, Ståhl S, Frejd FY (2010) Affibody molecules: engineered proteins for therapeutic, diagnostic and biotechnological applications. FEBS Lett 584:2670–2680
29. Majumdar S, Siahaan TJ (2012) Peptide-mediated targeted drug delivery. Med Res Rev 32:637–658
30. Ardeshirpour Y, Chernomordik V, Capala J, Hassan M, Zielinsky R, Griffiths G, Achilefu S, Smith P, Gandjbakhche A (2011) Using in-vivo fluorescence imaging in personalized cancer diagnostics and therapy, an image and treat paradigm. Technol Cancer Res Treat 10:549–560
31. You L, Wang X, Guo Z, Zhang D, Zhang P, Li J, Su X, Pan W, Zhang X (2018) MicroSPECT imaging of triple negative breast cancer cell tumor xenografted in athymic mice with radioiodinated anti-ICAM-1 monoclonal antibody. Appl Radiat Isot 139:20–25